Investigation of the high speed spinning process of poly(ethylene terephthalate) by means of synchrotron X-ray diffraction

R. Kolb[a,*], S. Seifert[b], N. Stribeck[b], H.G. Zachmann[b]

[a]*Exxon Research and Engineering Company, Route 22 East Annandale, NJ 08801, USA*
[b]*Institut fuer Technische und Makromolekulare Chemie, University of Hamburg, Hamburg, Germany*

Abstract

Measurements of wide-angle diffraction during high speed spinning of poly(ethylene terephthalate) (PET) have been performed using synchrotron radiation. The experimental set-up has been improved so that it became possible to determine the degree of crystallinity, crystallite orientation and fiber diameter along the spin line. For take-up speeds of 3600 m/min and higher, the crystal reflections appeared at a distance of 40 cm from the spinneret, just after the necking region. The crystallization speed increases proportional to increasing take-up speed. For the take-up speeds investigated, this results in a constant crystallinity profile when measured as a function of the distance from the spinneret. The final fibers exhibited an extraordinarily high degree of crystallinity, which has been attributed to the high molecular weight of the polymer. Below 3500 m/min, no crystallization and no necking could be detected up to a distance of 90 cm from the spinneret. The results showed that necking and crystallization were closely coupled. No orientation of the amorphous matrix prior to crystallization could be detected by means of X-ray diffraction. Moreover, the orientation of the crystallites was constant along the spin line. © 2000 Elsevier Science Ltd. All rights reserved.

Keywords: Poly(ethylene terephthalate); High speed spinning; Synchrotron wide-angle diffraction

1. Introduction

Synthetic fibers represent an important class of polymeric materials. The industrial production process of synthetic fibers, such as polyesters and polyamides, usually involves two steps. Initially, the fibers are melt spun at moderate take-up speeds of about 1000–1500 m/min. In a second step, the spun fibers are drawn and annealed to increase crystallinity and crystalline order. From an economical point of view, it is desirable to use a procedure, which generates highly oriented and crystalline fibers in one step. The concept of high speed spinning where spinning and drawing is combined provides such a one-step process. This process involves take-up speeds of up to 6000 m/min. During high speed spinning, one often finds a sudden decrease of the fiber diameter, which takes place close to the spinneret. This phenomenon is referred to as necking, and it is normally not observed during spinning at low take-up speeds. Perez and Lecluse were the first authors who reported a neck-like deformation during high-speed spinning [1]. Vassilatos et al. found a rapid increase of the birefringence and a temperature plateau in the vicinity of

the necking region [2]. They concluded that crystallization starts just after the onset of the necking region. Bansal and Shambaugh investigated the crystallization and the temperature during high speed spinning. By contrast, they did not find a temperature plateau up to take-up velocities of 5900 m/min, although crystallization started at that speed [3]. According to Kikutani et al. a neck cannot be defined sharply, but fluctuates over a narrow region along the spin line [4]. Moreover, Ziabicki pointed out that there is no definite criterion for the onset of such a phenomenon [5]. On-line studies of X-ray diffraction can be used to obtain additional information about the necking process and its correlation to other aspects of the structure forming processes, such as crystallization and the orientation behavior of the molecules. Therefore, this technique has been used extensively [6–10]. The first on-line studies during high speed spinning were performed by Haberkorn et al. who used a copper anode [12]. Because of its high intensity, synchrotron radiation is well suited for such real-time investigations [13–16]. Hirahata et al. have used synchrotron radiation to perform wide-angle diffraction experiments on poly(ethylene terephthalate) (PET) at take-up speeds up to 4000 m/min [13]. They developed a windowless set-up where the flight path of the X-ray beam contained helium in order to minimize the background

* Corresponding author. Tel.: +1-908-730-2970; fax: +1-908-730-3314.
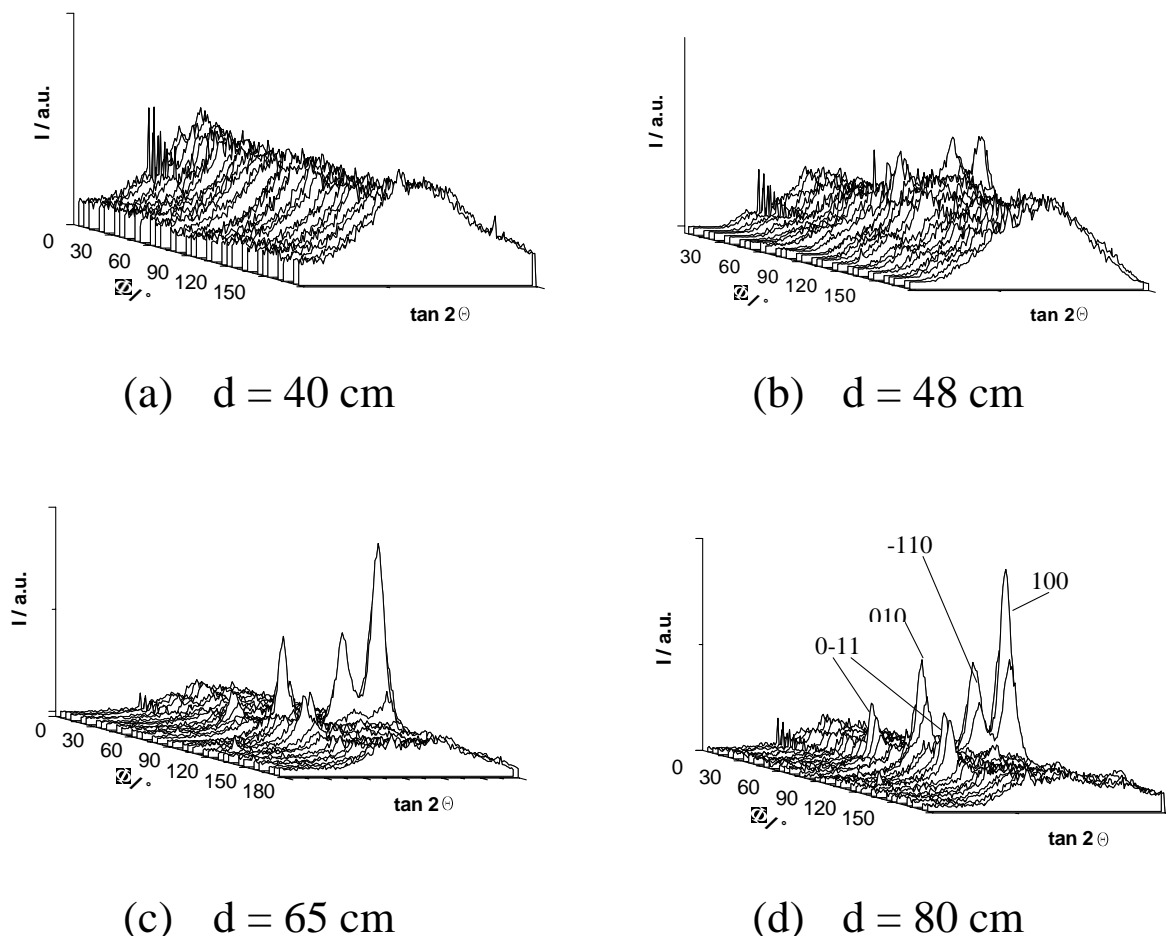*E-mail address:* rkolb@erenj.com (R. Kolb).

Fig. 1. Development of the wide-angle diffraction during spinning of PET at: (a) 40 cm; (b) 48 cm; (c) 65 cm; (d) 80 cm. (v = 4000 m/min). Radial cuts though the two-dimensional wide-angle patterns are shown.

scattering. The authors were able to detect the crystal reflections along the spin line. From separate measurements of the fiber diameter, they concluded that the crystallization starts at the beginning of the necking zone.

This present communication reports improvements of an experimental set-up and the results of a detailed study of the structure development of PET during high speed spinning. In particular, real time investigations of the wide-angle X-ray diffraction (WAXD) using synchrotron radiation are presented. This technique provides information about the crystallization rate and the development of the crystallite orientation. Moreover, the change of the scattering volume can be used as a relative measure of the fiber diameter.

2. Experimental

PET from Toyobo Co Ltd was used in the experiments. The material had a molecular weight of 80 000 g/mol and an intrinsic viscosity of 1.0 dl/g in p-chlorphenol/ tetrachlorethylene (60:40) at 30°C. Before extruding, the PET was dried for 16 h at 120°C in vacuum.

A single screw extruder, manufactured by Brabender,

Germany was used for this study. The screw had a diameter of 20 mm and a length of 280 mm. A metering pump kept the mass throughput at 10 g/min. A four-hole spinneret was used providing a throughput of 2.5 g/min per hole. The extruder assembly was mounted on a platform that could be moved vertically allowing WAXD measurements at varying distances from the spinneret ranging from 28 to 90 cm. The extruded fibers were taken up to a godet roll that enabled take-up velocities up to 4300 m/min. Further details of the spinning apparatus can be found elsewhere [13–15,17]. The spinning conditions were chosen according to Hirahata et al. The temperature at the die, T_D, and at the spin block, T_S, were 308 and 300°C, respectively [13]. The temperature gradient along the barrel was controlled by three heating zones T_3 = 290°C, T_2 = 275°C, and T_1 = 245°C.

The X-ray measurements were performed on the polymer beamline at the Hamburger Synchrotron Radiation Laboratory (HASYLAB) at the German Electron Synchotron (DESY) in Hamburg. The white synchrotron beam was monochromatized by reflection from a bent Ge (111) single crystal resulting in a wavelength of 0.15 nm. The primary beam intensity was measured by an ionization chamber and

the scattering intensity was normalized by dividing it by the intensity of the primary beam. The spot size at the sample position was $0.5 \times 1 \ mm^2$. A detailed description of the beamline can be found by Elsner et al. [23]. The accumulation time was 10 min per picture. After taking a diffraction pattern, a background picture was collected and subtracted from the diffraction pattern. In addition, the WAXD of the final fibers was measured in order to determine the degree of crystallization and the Hermans' orientation function of the specimen. Further, several measurements of the diameter of those fibers were done by means of a microscope in order to calibrate the integrated wide-angle scattering intensity.

Prior to analyzing the data for crystallinity and orientation, the scattering patterns were corrected for the decay of the primary beam and for background scattering. The degree of crystallinity, x_c, was calculated from an azimuthally averaged scattering curve by fitting an amorphous halo. This amorphous halo was obtained during spinning at lower distances from the spinneret. Assuming rotational symmetry of the specimen, x_c is given by

$$x_c = \frac{\int_0^\pi \int_{s0}^{s1} I_c(\mathbf{s}, \vartheta) \mathbf{s}^2 \sin \vartheta \ d\mathbf{s} \ d\vartheta}{\int_0^\pi \int_{s0}^{s1} I(\mathbf{s}, \vartheta) \mathbf{s}^2 \sin \vartheta \ d\mathbf{s} \ d\vartheta}$$

where I_C is the integrated intensity of the crystal reflections, I represents the scattering intensity of both the amorphous and the crystalline phases, and $\mathbf{s}$ is the scattering vector. The azimuthal distributions of the reflections have been used to calculate Hermans' orientation function, f, of the crystallites by applying Wilchinsky's method [24–26]. Because of the triclinic unit cell of PET, three equatorial reflections were necessary to calculate f. The Miller-indices of these reflections are (010), ($-$110), and (100) (see Fig. 1(d)).

The diffraction experiments were complicated by two factors: the fibers were vibrating horizontally so that a ceramic guide had to be used to keep them in the beam. More importantly, the diameter of a single fiber was only 25 μm at the onset position of crystallization. Therefore, the scattering from the polymer fiber was very weak compared to the background scattering. Hirahata et al. overcame this problem by removing all windows and filling the tube with helium in order to avoid scattering caused by the windows and the air [13]. However, that set-up required the use of metal apertures, which gave rise to strong equatorial scattering. The authors were able to detect the reflections from the crystallizing PET fiber, but their set-up did not allow detection of the amorphous halo. Moreover, it was not possible to perform quantitative measurements of the crystallinity and the crystallite orientation along the spin line.

This communication presents results of experiments, where the helium chamber was replaced by a vacuum recipient. The entrance of this vacuum recipient and the exit of the beam pipe were sealed with very thin poly(ethylene naphthalene dicarboxylate) (PEN) windows having a thickness of 2 μm.

The total intensity of the wide-angle diffraction pattern of the fibers was used as a relative value of the scattering volume. Ruland et al. have demonstrated that the scattering power of a semicrystalline polymer depends only on the scattering volume [18,19]. This method, however, involves an integration of scattering intensities ranging over the whole reciprocal space from $\mathbf{s} = 0$ to $\mathbf{s} = \infty$, which was impossible with the given set-up. Gehrke et al. have shown that for PET the intensity over the reciprocal space ranging from $\mathbf{s} = 1$ to $\mathbf{s} = 3$ is independent from the orientation and the degree of crystallinity of the molecules [19–21]. For a wavelength of $\lambda = 0.15$ nm this corresponds to an angular range of $2\theta = 8.6–26°$. This region was accessible with the present experimental set-up. Thus, assuming that the scattered intensity is independent of the structure of the system, the integrated wide-angle scattering intensity could be used to determine the fiber diameter. The advantage of this method is that the fiber diameter can be measured simultaneously with the wide-angle scattering. Moreover, from one single picture the crystallinity, the orientation of the polymer chains, and the fiber diameter can be determined [17,22]. To calculate the integrated intensity, the detector counts of the fully corrected scattering pattern have been integrated over the azimuthal angle ϕ (assuming fiber symmetry) and over the scattering angle θ. This intensity is proportional to the scattering volume. After calibrating the intensity with a fiber of a known diameter, the fiber diameter along the spin line could be measured.

3. Results and discussion

Fig. 1 shows an example of the development of the crystal reflections along the spin line at a take-up speed of 4000 m/min. The curves represent radial cuts through the two-dimensional wide-angle patterns at different azimuthal angles ranging from $\phi = 0°$ to $\phi = 180°$. (It is to be noted that the data were not smoothed or otherwise manipulated; only the corrections described in the experimental part have been applied.) At a distance of 30 cm, one can see an isotropic amorphous halo. A few centimeters down the spin line, at 45 cm, the WAXD pattern shows very weak reflections (Fig. 1 (b)), which are highly oriented indicating the onset of crystallization. The WAXD patterns taken at higher distances from the spinneret show an increase in the reflection intensity as the crystallization continues. The Miller indices of the reflections are given in Fig. 1(d). Further, it can be seen that the azimuthal width of the reflections did not practically change during the course of crystallization. Similar patterns have been obtained for the spinning speeds of 3600, 3800 and 4200 m/min. At a take-up speed of 3500 m/min and below, no crystallization could be observed up to a distance of 90 cm. The two-dimensional scattering
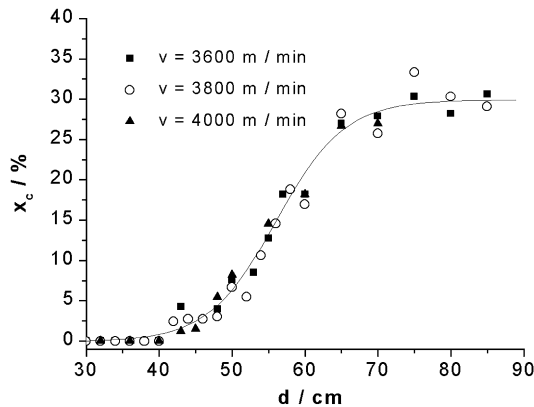
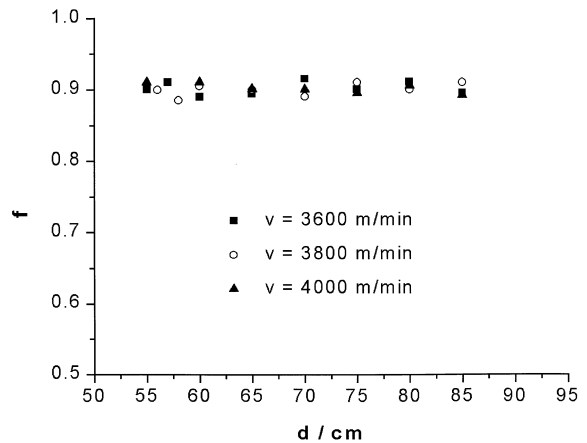Fig. 2. x_c as a function of the distance from the spinneret at three take-up velocities and a sigmoidal fit of the data obtained at 3800 m/min.

Fig. 3. Hermans' orientation function, f, as a function of the distance from the spinneret at different take-up velocities.

patterns in Fig. 1 show that oriented crystals grew from an apparently unoriented amorphous matrix. Moreover, the orientation of the crystallites did not change along the spin line. These results are in good agreement with previous investigations [11,17,27]. Fig. 2 shows the degree of crystallinity, x_c, as a function of the distance from the spinneret at three different take-up velocities. The solid line is a sigmoidal fit of the data obtained at 3800 m/min. A variation of the take-up speed between 3600 and 4200 m/min had no influence on the crystallization kinetics. Further, x_c of the final fibers in these three experiments was practically identical (see Table 1). The crystallization started at a distance of about 40 cm. The change of the onset position of crystallization as a function of the take-up speed is insignificant. The crystallization rate reached its maximum at a distance of about 56 cm. Up to a take-up speed of 4200 m/min the whole crystallization process occurred at distances between 30 and 90 cm, which corresponds to a crystallization time of 20 ms at $v = 4200$ m/min. The spun fibers showed an extraordinarily high degree of crystallinity as shown in Table 1. By contrast, Huisman and Heuvel found a degree of crystallinity of about 5% at comparable spinning conditions. Their experiments employed PET having a molecular weight of 25 000 g/mol [28]. Additionally, they performed spinning experiments up to take-up speeds of 6000 m/min. At this take-up speed, the final fiber had a degree of crystallinity of 24%. The

comparatively high value of x_c found in the present experiment is due to the high molecular weight. This explanation is in good agreement with Shimitzu's results, which reported that the degree of crystallinity increases with the molecular weight [29]. He attributed this effect to the higher stress resulting from higher melt viscosity.

Fig. 3 shows Hermans' orientation function, f, of the fiber as a function of the distance from the spinneret at three take-up velocities, v. The orientation of the crystallites developed during spinning was remarkably high. This can also be attributed to the high molecular weight. For take-up speeds ranging from 3600 to 4000 m/min, a value of 0.9 is found. Moreover, the orientation function of the crystallites is constant along the spin line for each take-up velocity. The orientation of the final fiber was the same as during spinning as shown in Table 1. The fact that the orientation of the crystallites does not change along the spin line has been reported in a number of publications [8,11,17,22]. It has been concluded that the nucleation process of the crystallization determines the degree of the crystallite alignment; a very small amount of highly elongated chain segments

Table 1
Degree of crystallinity, Hermans' orientation function, and fiber diameter during spinning and of the final fiber

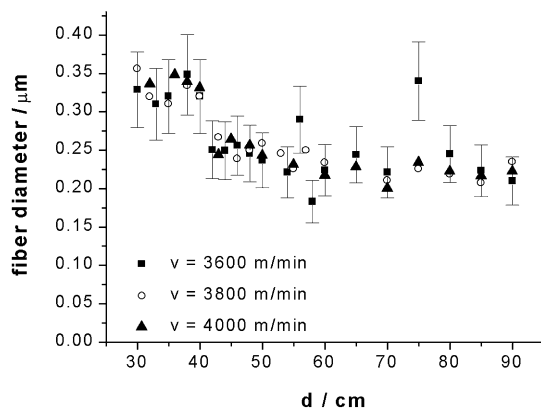|	Take-up speed				
	3500	3600	3800	4000	4200
x_c (75 cm) (%)	0	33.0	34.1	33.4	32.2
x_c (final fiber) (%)	0	36.5	34.9	36.1	35.0
f (75 cm)	0.91	0.89	0.90	0.89	0.89
f (final fiber)	0.91	0.91	0.89	0.89	0.89
D (75 cm) (μm)	27.2 ± 4	24.5 ± 4	21.9 ± 4	22.2 ± 4	24.1 ± 4
D (final fiber)/μm	26.0	26.2	26.1	26.0	25.9

Fig. 4. Integrated intensity of the WAXD pattern as a function of the distance from the spinneret.

exists in the melt prior to crystallization. These few regions of oriented polymer chains act as nuclei for the crystallization because of their higher order and density [11]. The amount of oriented chain segments is too small to be detected by X-ray diffraction.

Fig. 4 shows the fiber diameter derived form the integrated intensity of the WAXD pattern as a function of the distance from the spinneret. For take-up speeds higher than 3500 m/min, a sudden 25% decrease of the scattering volume occurred at distances of about 40 cm from the spinneret. This decrease corresponds to a reduction in the fiber diameter, D, of 14%, which clearly shows that a necking process took place. The uncertainty of the data points was significant as indicated by the error bars. However, the experiments have been repeated many times, and the reproducibility of the results is strong evidence for a decrease of the fiber diameter according to Fig. 4. Further, it can be seen that the necking region was extended over a range of about 4 cm along the spin line ($d = 38$–42 cm). It must be noted that each data point represents an average over 10 min. It can, therefore, not be concluded that the length of the neck was 4 cm. It could also be possible that a more sharply defined neck fluctuates over a range of 3–4 cm as suggested by Haberkorn et al. [12] and Hirahata et al. [13]. A comparison of the onset of crystallization and the position of the necking region clearly shows that both phenomena accompanied each other. Presently, there is disagreement about where crystallization starts with respect to the neck. Results from Hirahata et al. seem to indicate that crystallization starts before or at the beginning of the necking zone [13]. In contrast, both Kikutani et al. and Haberkorn et al. suggested that crystallization starts further down the spin line as a consequence of the necking process [4,12]. It must be noted, however, that crystal reflections can only be detected when x_c exceeds 5%. This is due to the small crystallite size and the strong thermal fluctuations at the beginning of crystallization. Therefore, it cannot be concluded from the WAXD measurements that the crystallization starts beyond the necking region.

4. Conclusions

Within the series of performed high-speed spinning experiments at constant feed, the take-up speed was varied in a broad interval. Above a threshold take-up speed, necking is observed at a position only 40 cm behind the spinneret, which goes along with the onset of crystallization. Thereafter, a crystallinity profile can be recorded as a function of the distance from the spinneret. As shown in Fig. 4, further increase of the take-up speed does not change shape and position of this profile. From this finding of a master curve, it can be concluded that crystallization velocity is closely coupled to the take-up speed in the spinning experiment. Moreover, this finding may be useful for future technical application. Any device capable of altering the process of structure formation could be put at a fixed position behind the spinneret. Related to the process of high-speed spinning such a position defines a specific degree of crystallinity, which is independent from the take-up speed.

References

[1] Perez G, Lacluse C. Proc. 18th Int. Man-Made Fiber Conf., Dornbirn, Austria, 1979.
[2] Vassilatos G, Knox BH, Frankfort HRE. High speed fiber spinning, New York: Wiley Interscience, 1985.
[3] Bansal V, Shambaugh RL. Polym Engng Sci 1998;38(12):1959.
[4] Kikutani A, Matsui M. High speed fiber spinning, New York: Wiley Interscience, 1985.
[5] Ziabicki A. High speed fiber spinning, New York: Wiley Interscience, 1985.
[6] Fung PYF, Orlando E, Carr SH. Polym Engng Sci 1973;13:295.
[7] Kitao T. J Polym Sci, Polym Phys Edu 1973;2:1091.
[8] Spruiell JE, White JL. Polym Engng Sci 1975;15:660.
[9] Nadella HP, Henson HM, Spruiell JE, White JL. J Appl Polym Sci 1977;21:3003.
[10] Katayama K, Amano T, Nakamura K. Kolloid Z Z Polym 1968;226:125.
[11] Cakmak M, Teitge A, Zachmann HG, White JL. J Polym Sci B, Polym Phys 1993;31:371.
[12] Haberkorn H, Hahn K, Breuer H, Dorrer H-D, Matthies P. J Appl Polym Sci 1993;47:1551.
[13] Hirahata H, Seifert S, Zachmann HG, Yabuki K. Polymer 1996;37(23):5131.
[14] Hsiao BS, Kennedy AD, Leach R, Barton Jr, Harlow R, Ross R, Seifert S, Zachmann HG. ACS Polym Prep 1995;36(1):340.
[15] Samon MS, Schultz JM, Wu J, Hsiao B, Yeh F, Kolb R. J Polym Sci B, Polym Phys 1999;37:1277.
[16] Bras W, Ryan AJ. J Appl Cryst 1997;37:1277.
[17] Kolb R, Seifert S, Stribeck N, Zachmann HG. Polymer 1999 in press.
[18] Ruland W. Acta Cryst 1961;14:1180.
[19] Ruland W. Faser und Textiltechnik 1960;15(11):533–537.
[20] Gehrke R. Dissertation. University of Hamburg, 1985.
[21] Gehrke R, Zachmann HG. Macromol Chem 1985;182:627.
[22] Kolb R. Dissertation. University of Hamburg, 1997.
[23] Elsner G, Riekel C, Zachmann HG. Adv Polym Sci 1985;67:1.
[24] Hermans PH, Hermans JJ, Vermaas D, Weidinger A. J Polym Sci 1947;3:1.
[25] Hermans PH, DeBooys JJ. Kolloid-Z 1939;88:73.
[26] Wilchinsky ZW. J Appl Phys 1960;31:1969.
[27] Zachmann HG. Proc. 18th Int. Man-Made Fiber Conf. Dornbirn, Austria, 1979.
[28] Huisman R, Heuvel HM. High speed fiber spinning, New York: Wiley Interscience, 1985.
[29] Shimitzu J. High speed fiber spinning, New York: Wiley Interscience, 1985.